Progress In Electromagnetics Research C, Vol. 131, 73–87, 2023

Four Element UWB MIMO Antenna with Improved Isolation Using Resistance Loaded Stub for S, C, and X Band Applications

Sumit K. Gupta[1, *], Robert Mark[2], Kaushik Mandal[3], and Soma Das[1]

Abstract—This article proposes a four-port multiple input multiple output (MIMO) ultra-wideband (UWB) antenna that operates across 3 to 13 GHz. Four identical fractal patches are placed orthogonally to each other. The uniqueness of the proposed design is that it does not need to incorporate any dedicated/specific design/component to realize notches within the UWB range. The elimination of notches, enhancement of bandwidth, and improvement of isolation have been achieved by integrating a resistance-loaded stub with the ground plane. The isolation between the elements was measured to be below −20 dB across the entire operating band. The fabricated prototype exhibits better diversity parameters like envelop correlation coefficient (ECC) < 0.003, diversity gain (DG) > 9.99, channel capacity loss (CCL) < 0.4 bps/Hz, and mean effective gain (MEG) < 2 dB. The proposed MIMO antenna shows omnidirectional radiation patterns with a peak gain of 5.4 dBi and radiation efficiency $> 66\%$ with required compactness having interelement (edge to edge) distance of 5.4 mm. After application of decoupling method radiation efficiency varies from 66% to 82% with gain ranging between 1.8 and 5.54 dBi. The diverse performance of the fabricated MIMO proves it to be a good candidate for UBW imaging, LTE applications, and S, C, and X band applications.

1. INTRODUCTION

In wireless communication system, the increased number and quality of applications lead to the requirement of ultra-wideband (UWB) antennas which can fulfil the requirements with increased data rate [1]. The design of UWB characteristics with size miniaturization is a challenge for researchers. Different techniques like composite left/right-handed transmission-line with E shaped slots [2], metamaterial based H shaped and T shaped slits with spiral ground [3, 4], etching F and T shaped slits on the ground plane and radiating patch [5], L- and F-shaped radiation cells-based metamaterial-based transmission line along with spirals [6], L & C integrated composite left/ right hand metamaterial based planar antenna [7–9], circularly polarized antenna with different feeding techniques [10], foldable bowtie shaped self-grounded structure [11, 12], etc. are typical examples which are proposed to achieve UWB characteristics in recent findings.

Again, the use of multiple-input multiple-output (MIMO) configuration is also suggested in recent literatures to achieve UWB characteristics along with enhanced data transmission rate, reduced multipath fading, and good diversity performance [13–16]. The use of MIMO antenna gives advantages of system reliability, channel capacity, and diversity performances; however, the use of multiple antennas with required compactness causes the system to suffer from mutual coupling between closely placed antenna elements. Several techniques have been presented to reduce mutual coupling without changing other desired antenna parameters (gain, channel capacity, etc.) appreciably [17–20] like metamaterial

Received 5 December 2022, Accepted 28 February 2023, Scheduled 18 March 2023

* Corresponding author: Sumit Kumar Gupta (sgupta@ggu.ac.in).

[1] Department of ECE, Guru Ghasidas Vishwavidyalaya (Central University), Bilaspur, India. [2] DRDO-Microwave Tube Research and Development Centre, Bangalore, India. [3] Department of Electronics, Institute of Radiophysics and Electronics, Institute of Radiophysics and Electronics, India.

based super substrate [21, 22], U shaped intercoupled isolation wall [23], metamaterial based EM band gap [24], inserting slots in slot array antenna [25], stub loaded slot with split ring resonator (SRR) structure [26], curved stub with pattern diversity [27], defected ground structure (DGS) based monopole with notch and slit in ground along with U shaped stub [28], Sierpinski knop fractal UWB antenna with complementary split-ring resonator (CSRR) structure [29, 30], Minkowski fractal with DGS structure [31], metamaterial-based isolator [32, 33], etc.

The design of a 4 element MIMO antenna in recent literatures utilizes the technique of orthogonal placement of antenna elements along with different isolation designs to achieve required compactness like Koch fractal geometry [34], L-shaped stub in the ground plane [34, 35], U and H-shaped slots [36], T-C shaped slots with isolated ground [37], CSRR structures with isolated ground [38], fork shaped via loaded MIMO [39], polarization diversity and slit on the ground [40], octagonal Koch fractal shaped MIMO antenna [41], isolated ground with tuneable operation using capacitors, varactors and PIN diodes [42], inverted L shaped isolation structure [43], coplanar waveguide (CPW) fed MIMO with optimized gap between the antenna element and ground plane [44], etc.

Based on the literatures available and reviewed above, one can say that fractal geometry offers miniaturization because of its self-similar structure and space-filling properties. The space-filling structure changes the electrical path for the surface currents and gives the required advantage of fractal design. In this paper, hexagonal fractal geometry has been conceived because of its simplicity and good UWB response in comparison to the other structures. The antenna elements are placed strategically orthogonal to each other to accomplish isolation well below −15 dB. The proposed antenna without resistive stub exhibits wideband characteristics across 3–13 GHz with notches at 6.5–7.15 GHz and 8.05–9.12 GHz. These notches between the application bands help to reduce interference in the proposed ranges. A lumped resistance is used to connect a metallic stub with the partial ground plane of the basic hexagonal fractal-based UWB antenna. Tactical inclusion of this resistance-loaded stub helps in improving isolation, better impedance matching, as well as the reduction of notches. The proposed four-port MIMO antenna successfully offers better isolation by adopting the relatively simple approach.

2. FORMULATION AND DESIGN

2.1. Antenna Design

The proposed four port orthogonally placed MIMO design is shown in Figure 1. It is fabricated on a low-cost FR-4 substrate with the dimension of 93 mm × 93 mm × 1.6 mm, dielectric constant of 4.4, and

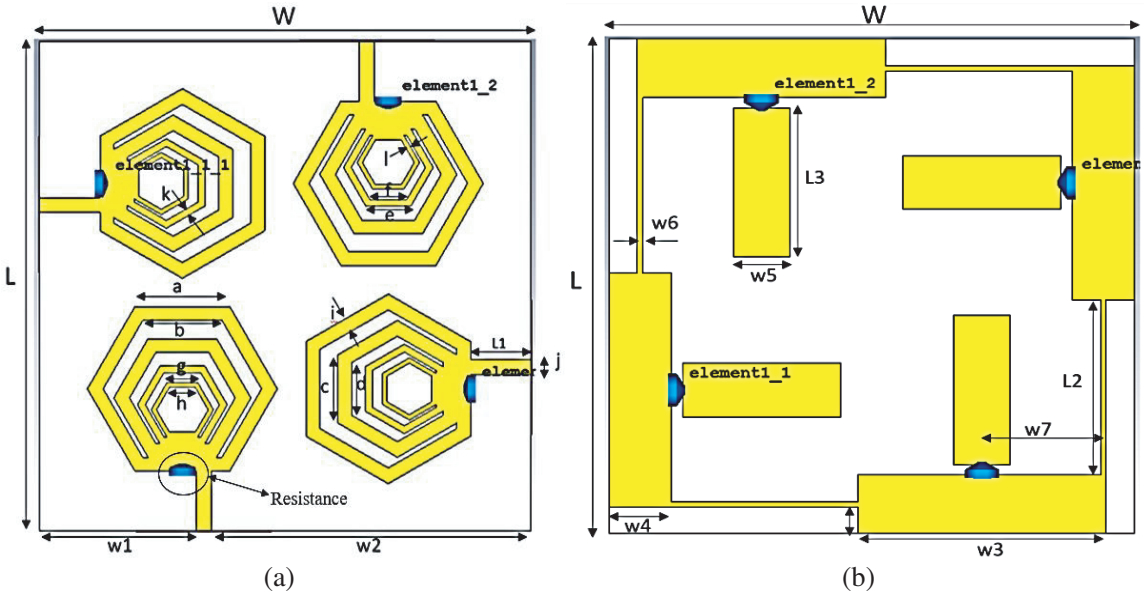

Figure 1. Four-element fractal UWB MIMO antenna. (a) Front view. (b) Back view.

loss tangent of 0.02. The ground plane on the back side of the substrate is connected with resistance loaded stub to achieve mutual coupling reduction and UWB response without notches. The ground of proposed design is connected with thin strips of copper as split ground is not practical in real system instead of common reference ground for MIMO.

The optimised design parameters, as shown in Figure 1, are $W = 93\,\text{mm}$, $L = 93\,\text{mm}$, $w1 = 29.66\,\text{mm}$, $w2 = 60.50$, $L1 = 11.41\,\text{mm}$, $a = 18\,\text{mm}$, $b = 15\,\text{mm}$, $c = 13\,\text{mm}$, $d = 10\,\text{mm}$, $e = 8.5\,\text{mm}$, $f = 7\,\text{mm}$, $g = 5.9\,\text{mm}$, $h = 4.9\,\text{mm}$, $i = 3\,\text{mm}$, $j = 2.84\,\text{mm}$, $k = 1.5\,\text{mm}$, $l = 1\,\text{mm}$, $w3 = 44\,\text{mm}$, $w4 = 11\,\text{mm}$, $w5 = 10\,\text{mm}$, $w6 = 1\,\text{mm}$, $w7 = 21\,\text{mm}$, $L2 = 33\,\text{mm}$, $L3 = 28\,\text{mm}$.

2.2. Design Evolution of Single Element UWB Antenna

During the initiation of the design, the widths of the strips of hexagon are taken as constant. The sides of a regular hexagon at various stages are related with log periodic concept [46]. Initiator was multiplied with scale factor to generate various stages, and the dimension of the ground plane and the gap between the strips were optimized to get multiband response [46]. To enhance the response of the design from multiband to wideband, the width of hexagon strips and the gap between them are further optimized with reduced ground to get UWB characteristics with better impedance matching as shown in Figures 2(a)–(e).

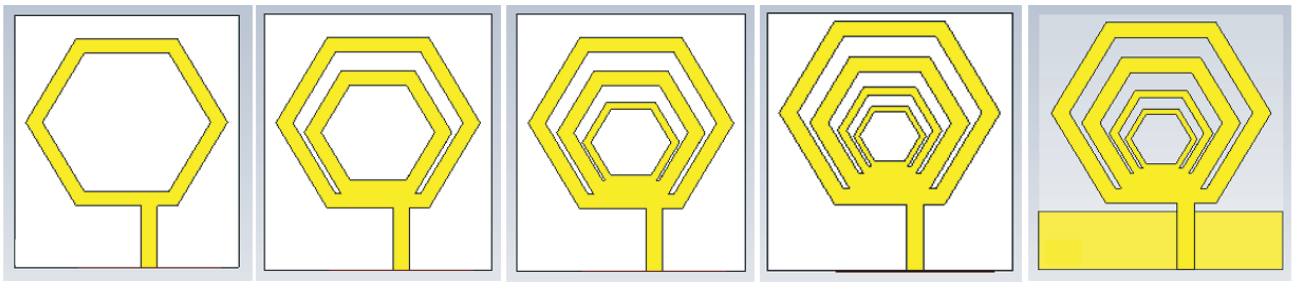

Figure 2. Evolution of single patch antenna with (a) initiator with full ground, (b) first fractal with full ground, (c) second Fractal with full ground, (d) third fractal with full ground, (e) final design with reduced ground.

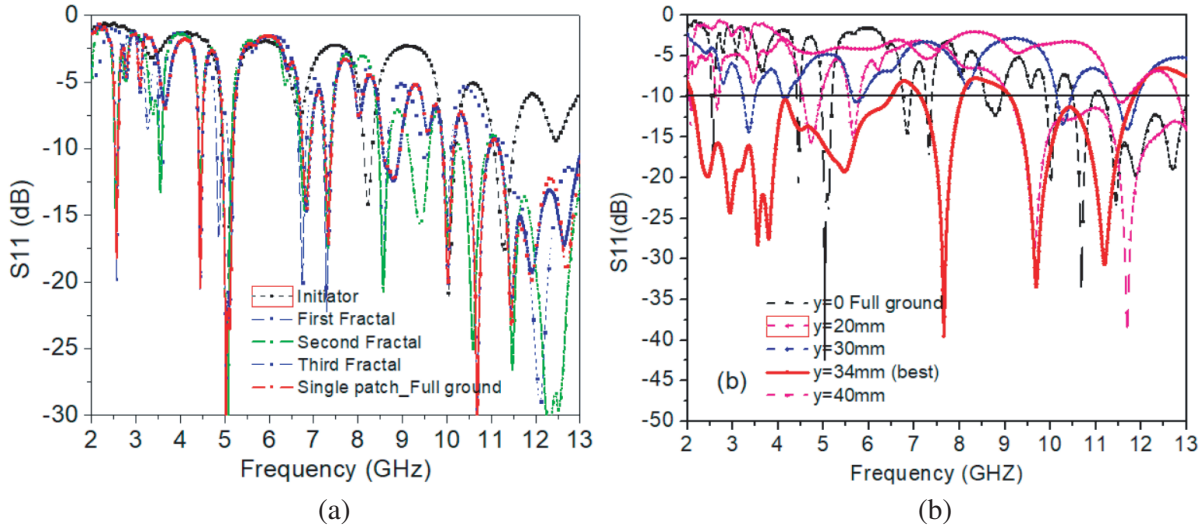

Figure 3. (a) Evolution of the final fractal with full ground. (b) Optimization of ground plane to get UWB response of the final fractal with ground reduction (y) from top.

Figure 3(a) gives the variation of reflection coefficient (S_{11}) characteristics for various iteration stages and for final design without any ground modification. The design with initiator resonates at four frequencies. The addition of each fractal hexagonal ring results in the addition of more resonating frequency in the lower side of the characteristics band. The addition of third fractal does not change any resonating frequency, but it gives better impedance matching. Along with the third fractal, the reduced ground plane also helps in creating extra resonating bands in between and causing multiband response to be converted to wideband response. Figure 3(b) shows the parametric optimization of the ground plane giving best results at $y = 34$ mm. Therefore, as per the design evolution and parametric variation in the ground (Figures 3(a)–(b)), the proposed single patch fractal gives UWB response from 2-13 GHz with two notch bands at 6.5–7.15 GHz and 8.05–9.12 GHz. This design is incorporated on low-cost FR-4 with the size of 44 mm × 40 mm as shown in Figure 2(e). This makes it a suitable candidate in the application range by extending its response for better diversity performance using MIMO technology.

2.3. Four Element MIMO Antenna without Resistance Loaded Stub in the Ground

Figures 4(a) and (b) show the front and back views of 4 element MIMO antenna where four radiating elements are placed orthogonal to each other which help to achieve reduced mutual coupling. The simulated S-parameter result of the 4 elements fractal MIMO antenna with connected reduced ground (Figure 4(b)) is shown in Figure 4(c), which gives wideband response with good isolation but still needs improvements at some resonating frequencies. The S_{11} response shows notches at 5–8 GHz range which needs to be addressed.

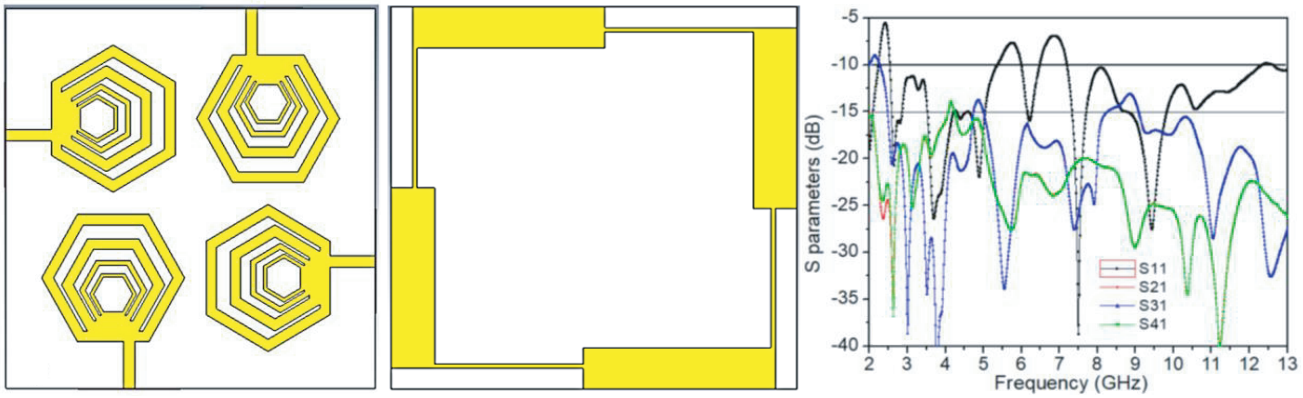

Figure 4. (a) Front view. (b) Back view. (c) S-parameters for 4-element fractal MIMO with connected reduced ground.

2.4. MIMO Antenna with Resistance Loaded Stub in the Ground

Based on the results obtained from 4-element fractal MIMO UWB antenna (Figure 4), the isolation and bandwidth of the designed antenna need improvement, and the same is obtained by further connecting resistance loaded stub in the ground plane. The S-parameter results for the parametric variation of the width of the stub (position of the stub is at the centre of the respective fractal) connected are given in Figures 5(a)–(d). As per the results shown, the best position is obtained at $stub_{var} = 4$ mm where $stub_{var}$ is the variation in the width of the stub (the final width of the stub is $w5 = 10$ mm).

Based on the results obtained in parametric variation of width of resistance loaded stub, the value of connecting resistance is then optimized, and the best value of the resistance obtained is $R = 100$ ohms. The parametric variations of the optimized results are shown in Figures 6(a)–(d). The desired improvement in bandwidth of the design is shown by removing the notches present in the single fractal patch. The optimized stub loaded with optimized resistance finally generates resonating bandwidth from 3 to 13 GHz with simulated isolation well below −15 dB for the full resonating band.

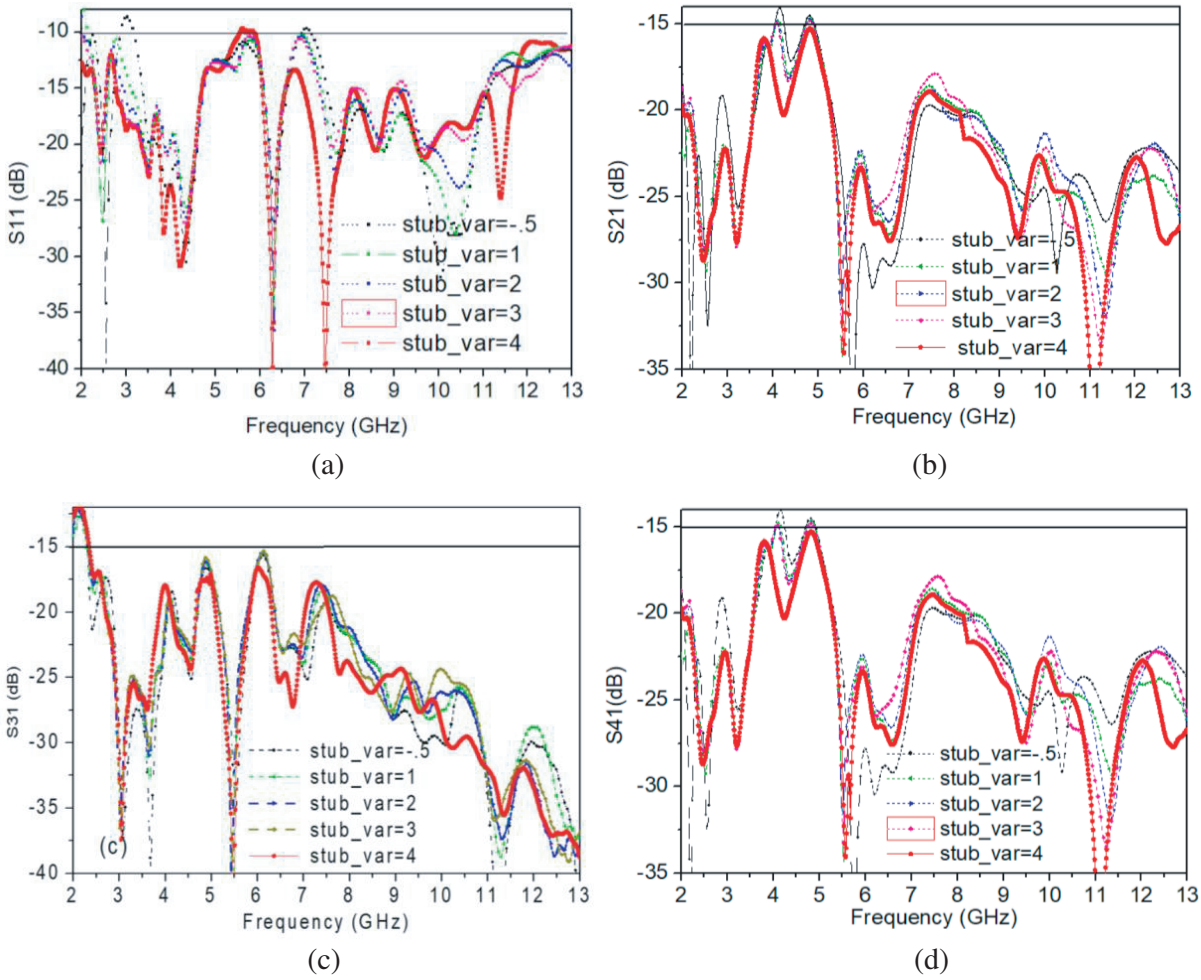

Figure 5. (a)–(d) Optimization of width of resistance loaded stub of 4 element fractal MIMO antenna.

As per the above discussion and variations in S parameters shown for the designs without stub and with stub, we can say that the application of a ground stub offers better impedance matching and improvement in isolation at certain frequencies to offer required isolation of below -15 dB throughout the resonating band (S_{11} below -10 dB). Surface current distributions without and with a stub are shown in Figure 7 at frequencies 3.83 GHz and 9.57 GHz.

3. EXPERIMENTAL VERIFICATION & RESULT ANALYSIS

The orthogonally placed 4-element fractal MIMO antenna with designed reduced ground is fabricated and tested in two port Agilent N5247Avector network analyser, as shown in Figures 8(a)–(c).

The measured results obtained are compared with simulated ones and are as shown in Figures 9(a) and (b). The measured results indicate good agreement with simulated ones. The comparison of simulated and measured S_{11} parameters and isolation parameters S_{21}, S_{31}, and S_{41} demonstrate that the fabricated antenna shows resonating frequency from 3 to 13 GHz with isolation below -20 dB as desired.

Figures 10(a)–(d) show the measured 2D radiation pattern of designed MIMO antenna in both E-plane and H-plane at four resonating frequencies: 3.83 GHz, 4.23 GHz, 8.57 GHz, and 11.37 GHz, respectively. As per the pattern obtained, the antenna offers omnidirectional radiation in both E-plane and H-plane. The low cross polarization, as observed in Figures 10(a)–(d) is also another desirable

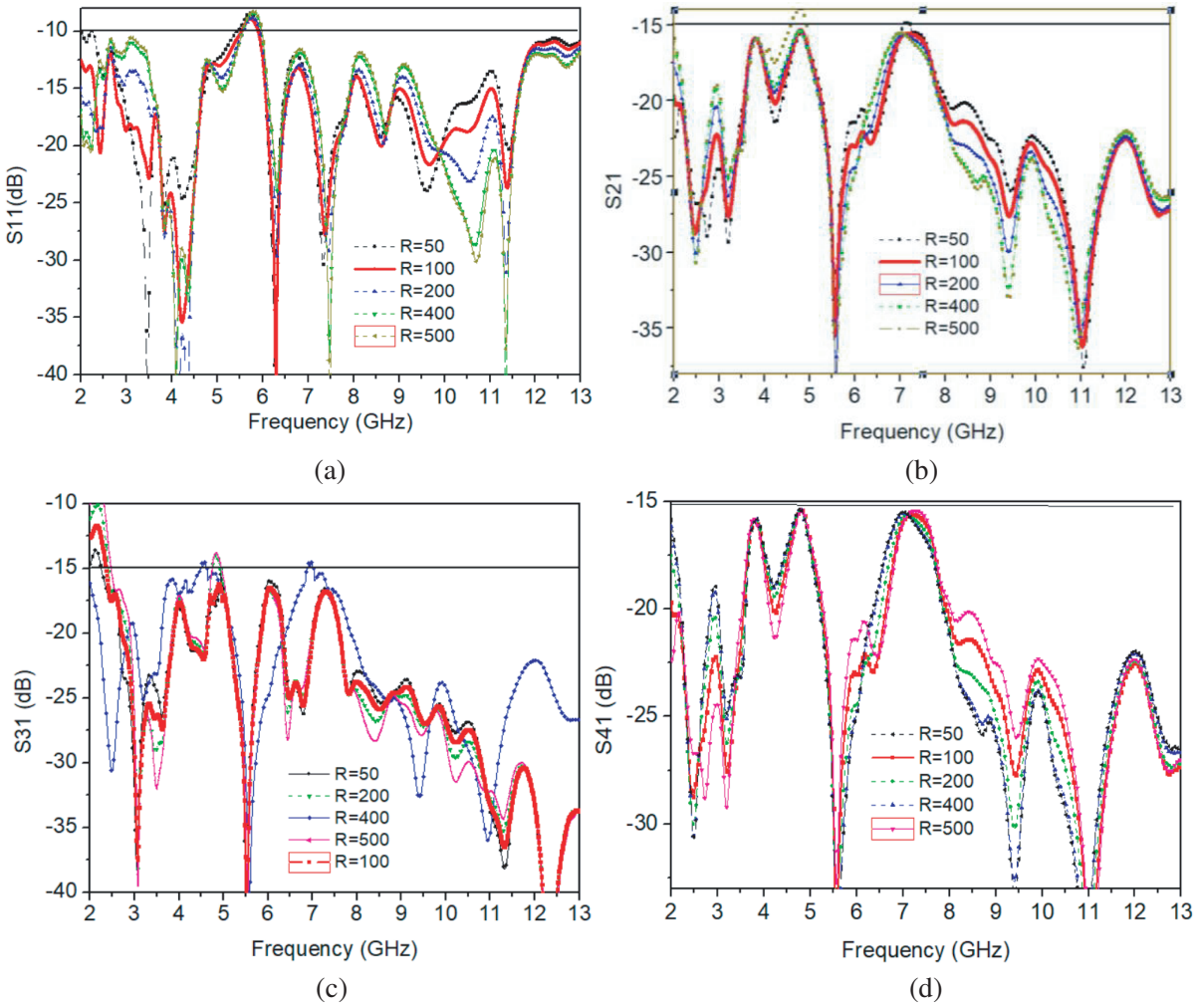

Figure 6. (a)–(d) Optimization of lumped element (resistance value) with S parameters at best stub position.

observation.

The mutual coupling effects of the proposed design are analysed by diversity parameters. The parameter envelop correlation coefficient (ECC) is one of the diversity parameters that shows the correlation between MIMO antenna elements calculated by using S parameters. A good ECC means that the multipath signal received in MIMO antenna is uncorrelated which finally results in a better signal to noise ratio at the receiver end and consequently in a better signal reception. The S-parameters alone could not be able to define whether ports are correlated or not. ECC does the same and gives complete diversity behaviour of MIMO antenna as given by:

$$\rho_{12} = \frac{\left|S_{11}^{*}S_{12} + S_{21}^{*}S_{22}\right|^{2}}{\left(1 - \left|S_{11}\right|^{2} - \left|S_{21}\right|^{2}\right)\left(1 - \left|S_{22}\right|^{2} - \left|S_{12}\right|^{2}\right)} \tag{1}$$

where S_{11} and S_{22} are return losses at port 1 and port 2 respectively. S_{21} and S_{12} are the isolation parameters between the antenna ports. In general, the value of ECC < 0.5 is considered to be good diversity performance [48]. Figure 11(a) shows the comparison of ECC values obtained using S parameters as well as from radiation field, and the results from both were found to be well below the acceptable limits of 0.5. The ECC values further prove that the designed antenna is an uncorrelated one.

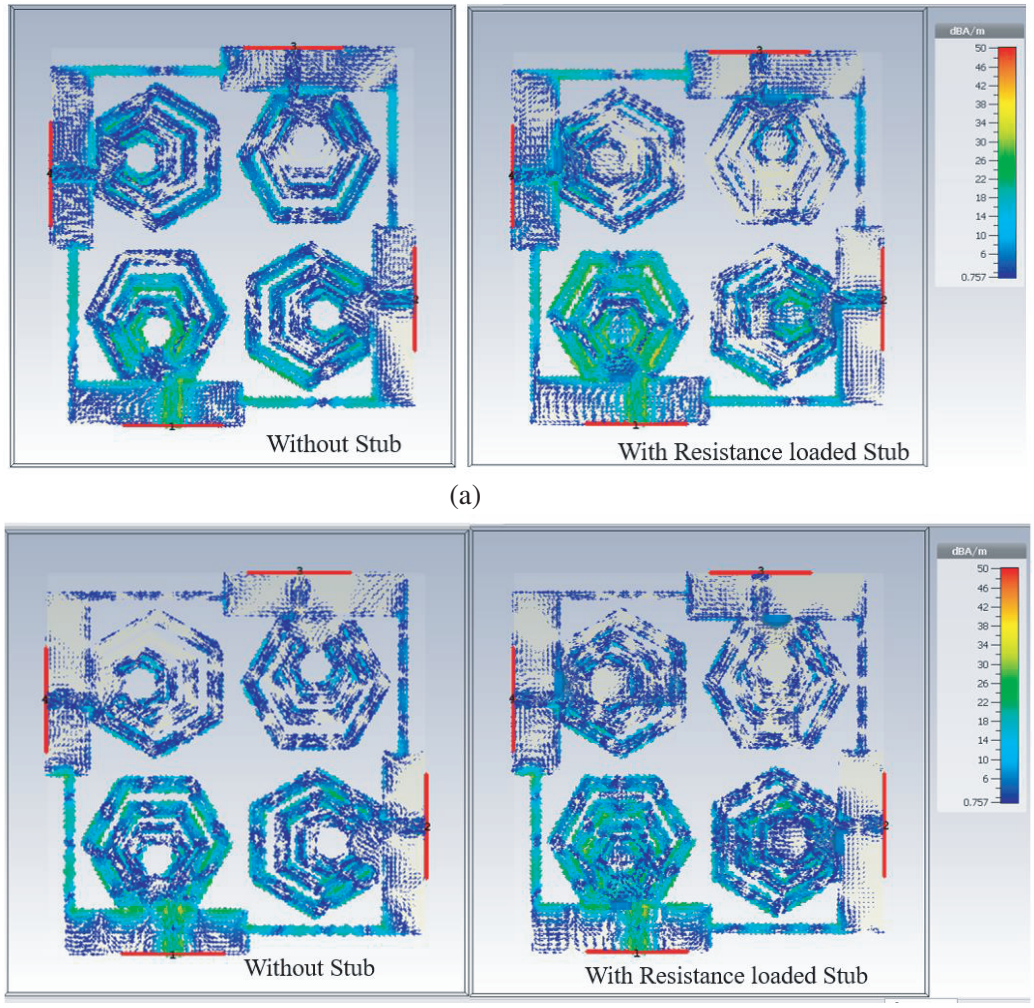

Figure 7. Surface currents without stub and with stub at (a) 3.83 GHz, (b) 9.67 GHz.

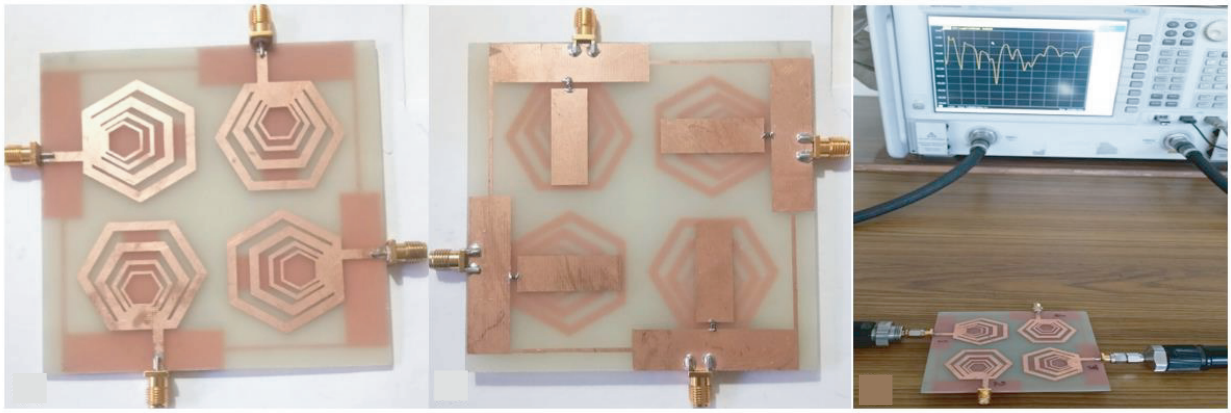

Figure 8. Fabricated 4-element MIMO. (a) Front view. (b) Back view. (c) Under testing using Vector Network Analyzer (VNA).

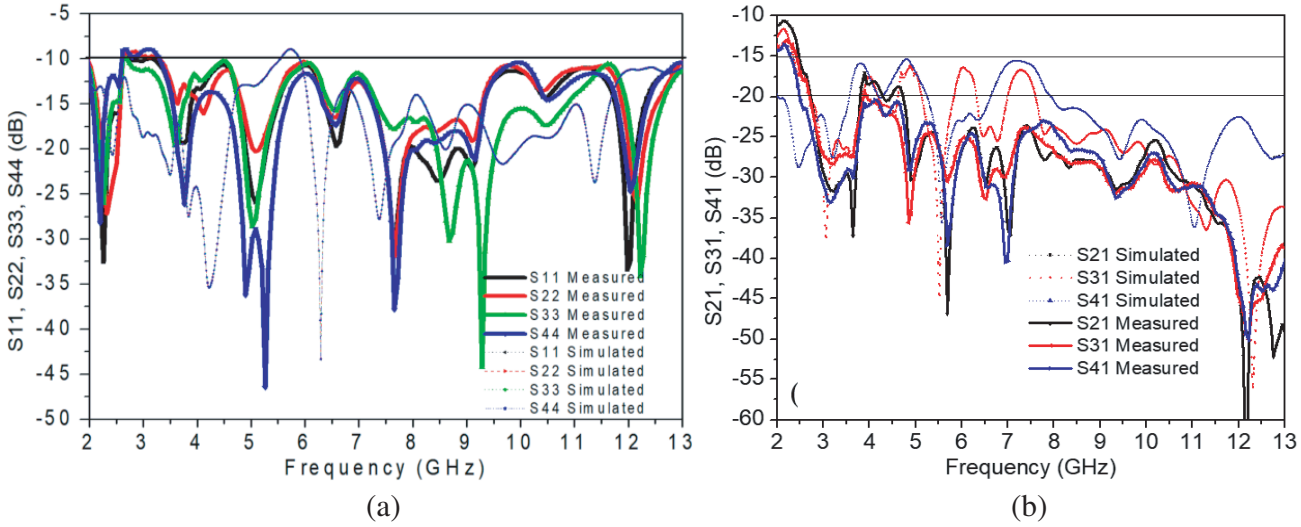

Figure 9. (a) Comparison of S_{11}, S_{22}, S_{33} and S_{44} (Simulated and Measured). (b) Comparison of S_{21}, S_{31}, S_{41} for (Simulated and Measured).

Another MIMO performance parameter is diversity gain (DG) which is a measure of average signal to noise ratio of all the signals transmitted by single antenna of MIMO and received via multiple paths at the receiver's end. Mathematical expression of diversity gain is given by:

$$Diversity\ Gain = \left[\frac{\gamma_c}{SNR_c} - \frac{\gamma_1}{SNR_1}\right]_{P(\gamma_c<\gamma_s/SNR)} \tag{2}$$

The diversity gain obtained for the present four port UWB MIMO antenna using radiation field and S parameters is shown in Figure 11(b). The DG calculated using measured S parameters is found to be > 9.99, and that from radiation pattern is > 9.80. These DG values in both cases further prove the better diversity performance and less channel capacity loss for the designed MIMO antenna than similar reference works.

The third MIMO performance parameter is total active reflection coefficient (TARC) which accounts for mutual coupling between the antenna elements and random phase signal combinations between ports, and it is mathematically defined as the ratio of square root of the total reflected power to the square root of total incident power [42]. The simulated TARC value was calculated in Computer Simulation Technology (CST) using random phase inputs, where phase varies between 0° and 180° to observe its effect on resonance of the antenna. Mathematically TARC is given by

$$\Gamma_a^t = \frac{\sum_{i=1}^{n} b_i^2}{\sum_{i=1}^{n} a_i^2}, \tag{3}$$

where a_i and b_i represent the incident and reflected signals, respectively.

The TARC was also calculated using measured S parameters, and the comparison of simulated and measured TARCs is shown in Figure 11(c). The TARC plot shows that there is no variation in resonance bandwidth when the input phase varies.

Another important MIMO performance parameter is channel capacity loss (CCL). CCL restricts the upper bound of the rate of information that can be fairly transmitted through the channel, and its value must be less than 0.4 bits/s/Hz for the MIMO system. CCL is calculated for designed MIMO systems using following equations [42]:

$$C_{loss} = -\log_2 \left|\psi^R\right| \tag{4}$$

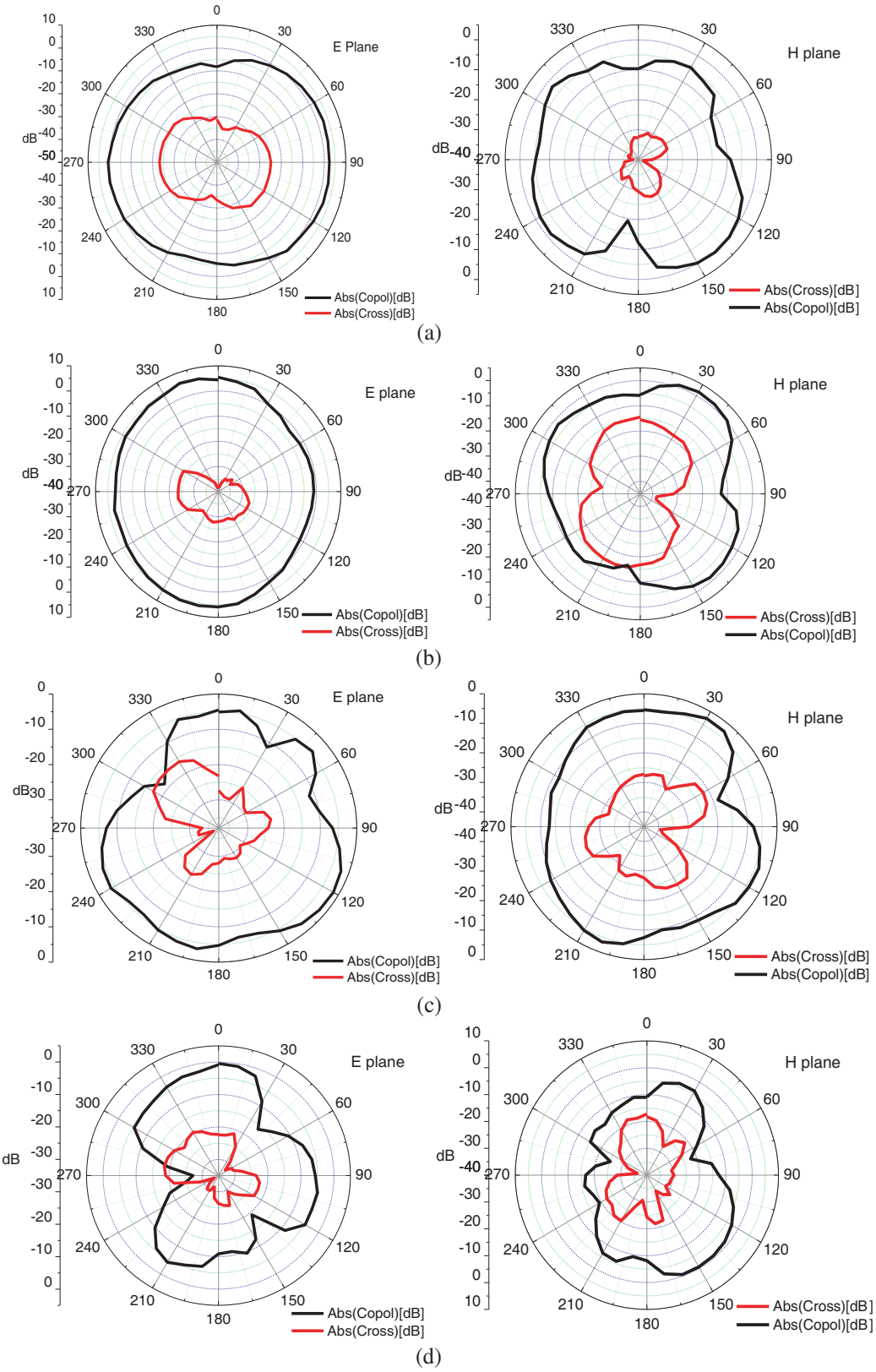

Figure 10. 4 element fractal MIMO antenna 2-D measured radiation pattern. (a) 3.83 GHz. (b) 4.23 GHz. (c) 8.57 GHz. (d) 11.37 GHz.

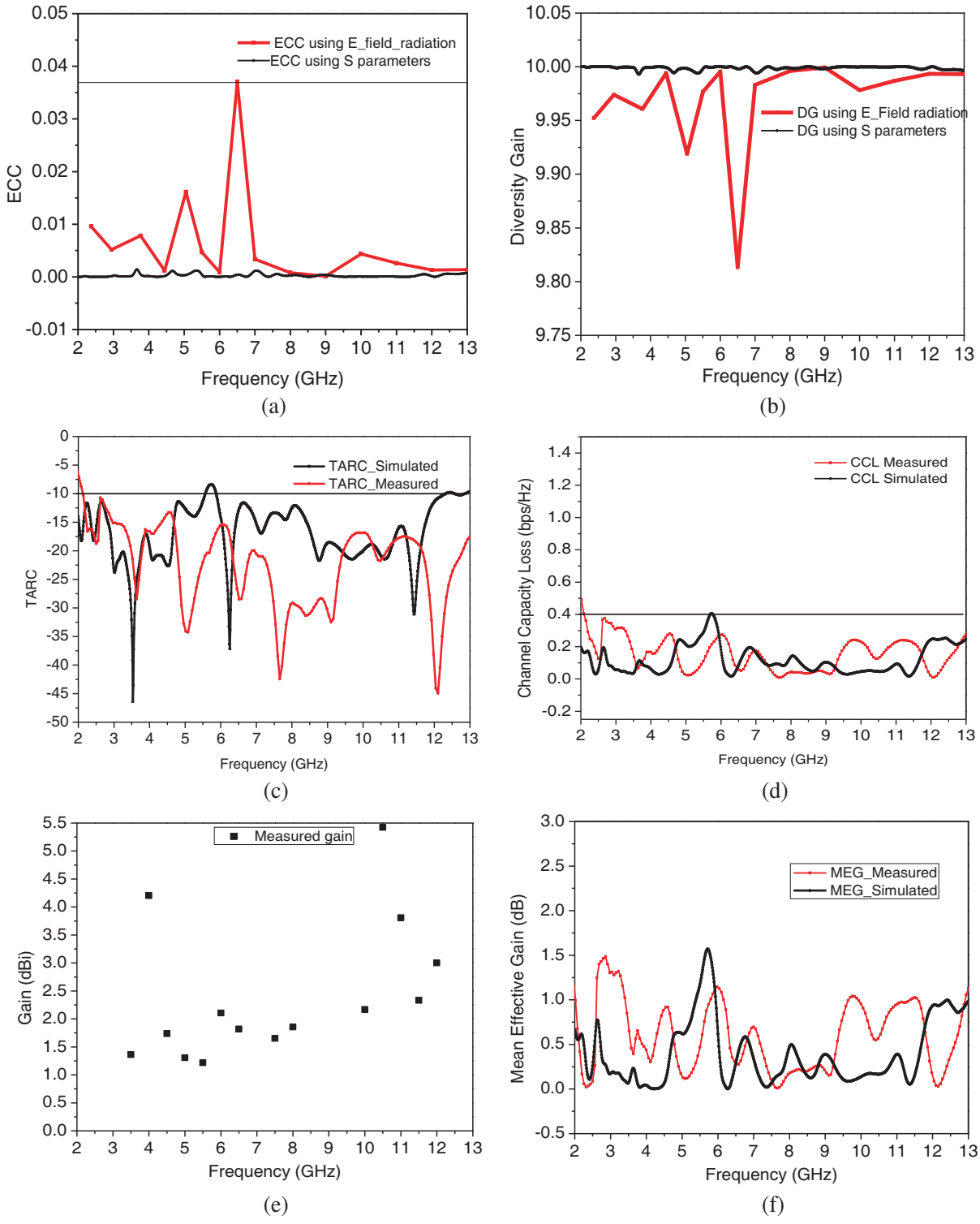

Figure 11. (a) Envelope correlation Coefficient. (b) Diversity gain. (c) Total active reflection coefficient. (d) Channel capacity Loss. (e) Gain (dBi). (f) Mean effective gain.

where ψ^R is the receiving antenna correlation matrix, given as

$$\psi^R = \begin{bmatrix} \varrho_{11} & \varrho_{12} \\ \varrho_{21} & \varrho_{22} \end{bmatrix} \tag{5}$$

$$\wp_{ii} = (1 - |S_{ii}|^2 - |S_{ij}|^2) \text{ and } \wp_{ij} = (S_{ii}^* S_{ij} + S_{ji}^* S_{ij}) \text{ for } i, j = 1 \text{ or } 2 \quad (6)$$

Figure 11(d) shows channel capacity loss characteristics for the proposed four port UWB MIMO antenna for simulated and measured values. It is seen that the value of the capacity loss is less than 0.4 bps/Hz for the resonating bands, which makes the antenna suitable for MIMO applications.

The gain of the fabricated antenna is calculated from measured radiated power and is obtained to be varying between 1.4 and 5.4 dBi for its resonating bandwidth. The scattered gain vs frequency plot is drawn in Figure 11(e).

Mean effective gain (MEG) is another parameter which is the measure of power received by the MIMO diversity antenna with respect to an isotropic antenna in the fading environment. It is calculated using the equation below

$$MEG_i = 0.5 \left(1 - \sum_{j=1}^{k} |S_{ij}|^2 \right) \quad (7)$$

Table 1. Comparison of the proposed work with published literature work with respect to parameters like size, bandwidth, measured gain, ECC, isolation.

Ref.	No. of element	applied design method	Size (mm) & Substrate	Operating Band (GHz) /BW (GHz)	Measured Gain (dBi)	Simulated Efficiency (%)	Diversity Gain	ECC	Isolation /Isolation improvement method	design complexity	Application Covered
[29]	4	Sierpinski Knopp fractal	40 mm ×40 mm FR-4	2.6–10.6 with notch at WiMax 3.5 GHz and WLAN 5.4 GHz regions.	Not reported (E plane H plane Co-Cross pole radiation pattern overlapping)	64	> 9.9 dB	< 0.07	< −20	CSRR slot with isolated ground	UWB MIMO applications
[31]	4	Minkowski fractal shaped DGS	80 mm ×80 mm FR-4	2.1–20 GHz with notch at 3.3–4.1, 8.2–8.6	Gain 3.5 dBi till 10 GHz then rises to 5.8 dBi at higher frequency range	80%	> 9.99	< .02	< −25	Yes, in the design/ optimization of fractal	UWB applications with stop bands for WiMAX and military /radar applications
[32]	4	Metasurface	40 mm ×40 mm FR-4	8.2–12 GHz	Peak gain 8.5 dBi	Maximum 76%	Not reported	Not reported	Better than −27 dB	Metamaerial unit cell with metal via	entire X-band
[36]	2 4	Fractal with C shaped slot	25 mm ×50 mm 50 mm ×50 mm Rogers	3.18–20.10 (notch at 3.51–4.25 and 5.06–5.92) 3.18–20.10 with notch at 3.42–4.23 and 4.95–6.04	Maximum 4.85 dBi	73%–90%	> 9.9	< 0.05	< −20 dB	Design of Koch geometry is complex	UWB: Imaging applications, X band RADAR applications & Ku band satellite system
[39]	4	CMA and vias and Fork-shaped	40 mm ×28 mm FR-4	3.05 to 13.05 GHz	Not reported	Not reported	Not reported	< 0.02	−17 dB	Multible stub and via are used	Suitable for UWB wireless communication
[41]	4	Koch Fractal UWB MIMO	45 mm ×45 mm FR-4	3–10.6 GHz excluding 5.5 GHz notch band.	Below 4 dBi upto 6 GHz Up to 4.5 dBi above 6 GHz	Not reported	Not reported	< 0.003	better than −17 dB/ grounded stubs	Design of Koch geometry is complex	Suitable for UWB wireless communication
[42]	4	Four port separate ground multipurpose filter circuit	109.2 mm ×109.2 mm Rogers RO4350	2.5–4.2 GHz,	more than 1.5 dBi in the working frequency	> 75%	Not reported	< 0.5	< −15 dB Multipurpose filter	Complex design with switches	sub-6 GHz 5G applications.
[45]	2	Metasurface isolating structure	60 mm ×40 mm FR-4	8.41–8.7 GHz 13.8–14.6 GHz 15.6–17.05 GHz 17.5–30 GHz	Maximum gain = 7.9 dBi	Not reported	Not reported	Not reported	Average improvement of 10 dB	Simple design with big antenna size	X, Ku, K, and Ka bands
[47]	4	Switchable filter is used	120 mm ×100 mm	2.5–4.2 GHz	2.3 dBi	> 65%	Not reported	< 0.01	−20 dB achieved	Diodes and complex circuits are designed	5G cognitive radio (CR) applications
This Work	**4 (Orthog-onally placed)**	**Fractal with resistance loaded stub in reduced ground**	**93 mm ×93 mm FR-4**	**3–13 GHz band**	**Peak gain = 5.4 dBi**	**> 66% Maximum = 82%**	**> 9.99 (Measured)**	**< 0.003 (Measured)**	**< −20 dB isolation for 3–13 GHz band**	**Simple to design and optimize**	**WLAN/LTE /C-band /X Band Applications**

where k represents the number of antennas, and i is the antenna under consideration for calculating mean effective gain. For better diversity performance, the MEG analysis of diversity antenna must give the ratio of MEG1/MEG2 to be below $< 3\,\text{dB}$ [49, 50]. The MEG of the proposed antenna is shown in Figure 11(f) for both simulated and measured values. The plot shows that the ratio MEG1/MEG2 is well below 3 dB for entire operating range of the designed antenna.

Table 1 shows the comparison of the proposed work with other reported literatures in terms of dimension, material, bandwidth, peak gain, diversity parameters, and application. The comparison shows that the proposed design offers relatively less complex design, large bandwidth, compact design, relatively better peak gain of 5.4 dBi with low-cost FR-4 material, and better diversity parameters like ECC, DG which give it upper hand in applications like UWB imaging, LTE applications, C, S, and X band applications.

4. CONCLUSION

In this paper, an orthogonally placed four port fractal MIMO antenna with UWB characteristics ranging from 3 to 13 GHz is presented. The proposed antenna is fabricated and tested for diversity parameters. The proposed design does not require any specific structure to create notches in between the application bands to reduce interference between them. For removal of the notches as well as for the bandwidth enhancement (continuous UWB) and isolation improvement, the resistance loaded stub is placed in the reduced ground plane. The measured isolation between the radiating elements is obtained to be $< -20\,\text{dB}$. The proposed MIMO antenna offers a peak gain of 5.4 dBi with stable radiation patterns in E plane and H plane. The investigation of diversity parameters like ECC (less than .003), DG (> 9.99), TARC, CCL ($< 0.4\,\text{bps/Hz}$), and MEG ($< 2\,\text{dB}$) were done from the measurement data, and the result proves that the designed MIMO antenna exhibits better diversity characteristics than its acceptable limits. The proposed UWB MIMO antenna proves to be a suitable candidate for applications like UWB imaging, LTE, S, C, and X bands, which range in 2–4 GHz, 6–8 GHz, and 8–12 GHz, respectively.

REFERENCES

1. Cicchetti, R., E. Miozzi, and O. Testa, "Wideband and UWB antennas for wireless applications: A comprehensive review," *International Journal of Antennas and Propagation*, Vol. 2017, Article ID 2390808, 45 pages, 2017.
2. Alibakhshi-Kenari, M., M. Naser-Moghadasi, R. Ali Sadeghzadeh, B. Singh Virdee, and E. Limiti, "New compact antenna based on simplified CRLH-TL for UWB wireless communication systems," *International Journal of RF and Microwave Computer-Aided Engineering*, Vol. 26, No. 3, 217–225, 2016.
3. Alibakhshi-Kenari, M., M. Naser-Moghadasi, R. Ali Sadeghzadeh, and B. Singh Virdee, "Metamaterial-based antennas for integration in UWB transceivers and portable microwave handsets," *International Journal of RF and Microwave Computer-Aided Engineering*, Vol. 26, No. 1, 88–96, 2016.
4. Alibakhshi-Kenari, M. and M. Naser-Moghadasi, "Novel UWB miniaturized integrated antenna based on CRLH metamaterial transmission lines," *AEU — International Journal of Electronics and Communications*, Vol. 69, No. 8, 1143–1149, 2015.
5. Sadeghzadeh, R. A., M. Alibakhshikenari, and M. Naser-Moghadasi, "UWB antenna based on SCRLH-TLs for portable wireless devices," *Microwave and Optical Technology Letters*, Vol. 58, No. 1, 69–71, 2016.
6. Sadeghzadeh, R. A., M. Alibakhshi-Kenari, and M. Naser-Moghadasi, 2015, "Composite right-left-handed-based antenna with wide applications in very-high frequency-ultra-high frequency bands for radio transceivers," *IET Microwaves, Antennas & Propagation*, Vol. 9, No. 15, 1713–1726, December 10, 2015.
7. Alibakhshi Kenari, M., 2013, "Design and modeling of new UWB metamaterial planar cavity antennas with shrinking of the physical size for modern transceivers," *International Journal of Antennas and Propagation*, 1–12, 2013.

8. Alibakhshikenari, M., B. S. Virdee, L. Azpilicueta, et al., "A comprehensive survey of "metamaterial transmission-line based antennas: Design, challenges, and applications"," *IEEE Access*, Vol. 8, 144778–144808, 2020.
9. Alibakhshikenari, M., E. M. Ali, M. Soruri, et al., "A comprehensive survey on antennas on-chip based on metamaterial, metasurface, and substrate integrated waveguide principles for millimeter-waves and terahertz integrated circuits and systems," *IEEE Access*, Vol. 10, 3668–3692, 2022.
10. Nadeem, I., M. Alibakhshikenari, F. Babaeian, et al., "A comprehensive survey on "circular polarized antennas" for existing and emerging wireless communication technologies," *Journal of Physics D: Applied Physics*, Vol. 55, No. 3, 033002, October 18, 2021.
11. Alibakhshikenari, M., B. S. Virdee, C. H. See, et al., "Dual-polarized highly folded bowtie antenna with slotted self-grounded structure for sub-6 GHz 5G applications," *IEEE Transactions on Antennas and Propagation*, Vol. 70, No. 4, 3028–3033, April 2022.
12. Alibakhshikenari, M., S. M. Moghaddam, A. Uz Zaman, J. Yang, B. S. Virdee, and E. Limiti, "Wideband sub-6 GHz self-grounded bow-tie antenna with new feeding mechanism for 5G communication systems," *2019 13th European Conference on Antennas and Propagation (EuCAP)*, 1–4, 2019.
13. Kowalewski, J., J. Eisenbeis, M. Tingulstad, Z. Kollar, and T. Zwick, "Design method for capacity enhancement of pattern-reconfigurable MIMO vehicular antennas," *IEEE Antennas Wirel. Propag. Lett.*, Vol. 18, 2557–2561, 2019.
14. Vasu Babu, K. and B. Anuradha, "Design of Wang shape neutralization line antenna to reduce the mutual coupling in MIMO antennas," *Analog. Integr. Circ. Sig. Process.*, Vol. 101, 67–76, 2019.
15. Gorai, A., A. Dasgupta, and R. Ghatak, "A compact quasi-self-complementary dual band notched UWB MIMO antenna with enhanced isolation using Hilbert fractal slot," *International Journal of Electronics and Communications*, 2018.
16. Mohanty, A. and S. Sahu. "High isolation two-port compact MIMO fractal antenna with Wi-Max and X-band suppression characteristics," *International Journal of RF and Microwave Computer-Aided Engineering*, Vol. 30, 1–11, 2019.
17. Singh, H. S., G. K. Pandey, P. K. Bharti, and M. K. Meshram, "Design and performance investigation of a low-profile MIMO/diversity antenna for WLAN/WiMAX/HIPERLAN applications with high isolation," *Int. J. RF Microw.*, Vol. 25, 510–521, 2015.
18. Kumar, A., A. Q. Ansari, B. K. Kanaujia, and J. Kishor, "High isolation compact fourport MIMO antenna loaded with CSRR for multiband applications," *Frequenz*, Vol. 72, 415–427, 2018.
19. Chouhan, S., D. K. Panda, V. S. Kushwah, and S. Singhal, "Spider-shaped fractal MIMO antenna for LAN/WiMAX/Wi-Fi/Bluetooth/C-band applications," *AEU — International Journal of Electronics and Communications*, Vol. 110, 152871, 2019, ISSN 1434-8411.
20. Sree, G. N. J. and S. Nelaturi, "Design and experimental verification of fractal based MIMO antenna for lower sub 6-GHz 5G applications," *AEU — International Journal of Electronics and Communications*, Vol. 137, 153797, 2021, ISSN 1434-8411.
21. Alibakhshikenari, M., A. Salvucci, G. Polli, et al., "Mutual coupling reduction using metamaterial supersubstrate for high performance & densely packed planar phased arrays," *2018 22nd International Microwave and Radar Conference (MIKON)*, 675–678, 2018.
22. Alibakhshikenari, M., B. S. Virdee, and E. Limiti, 2018, "A technique to suppress mutual coupling in densely packed antenna arrays using metamaterial supersubstrate," *12th European Conference on Antennas and Propagation (EuCAP 2018)*, London, UK, April 9–13, 2018.
23. Alibakhshikenari, M., B. S. Virdee, C. H. See, R. A. Abd-Alhameed, F. Falcone, and E. Limiti, 2018, "Array antenna for synthetic aperture radar operating in X and Ku-bands: A study to enhance isolation between radiation elements," 1083–1087, Aachen, Germany, June 4–7, 2018.
24. Alibakhshikenari, M., M. Vittori, S. Colangeli, et al., "EM isolation enhancement based on metamaterial concept in antenna array system to support full-duplex application," *2017 IEEE Asia Pacific Microwave Conference (APMC)*, 740–742, 2017.

25. Alibakhshikenari, M., B. S. Virdee, C. H. See, R. Abd-Alhameed, F. Falcone, and E. Limiti, "A new waveguide slot array antenna with high isolation and high antenna bandwidth operation on Ku- and K-bands for radar and MIMO systems," *2018 15th European Radar Conference (EuRAD)*, 401–404, 2018.
26. Bukkawar, S. and V. Ahmed, "Compact slot-loaded ultra-wideband multiple input multiple-output antenna with fractal inspired isolator," *Int. J. RF Microw. Comput. Aided Eng.*, e22036, 2019.
27. Biswal, S. P. and S. Das, "A compact printed ultra-wideband multiple-input multiple output prototype with band-notch ability for WiMAX, LTEband43, and WLAN systems," *Int. J. RF Microw. Comput. Aided Eng.*, e21673, 2019.
28. Hasan, M. N., S. Chu, and S. Bashir, "A DGS monopole antenna loaded with U-shape stub for UWB MIMO applications," *Microw. Opt. Technol. Lett.*, 1–9, 2019.
29. Rajkumar, S., K. T. Selvan, and P. H. Rao, "Compact 4 element Sierpinski Knopp fractal UWB MIMO antenna with dual band notch," *Microw. Opt. Technol. Lett.*, Vol. 60, 1023–1030, 2018.
30. Gurjar, R., D. K. Upadhyay, B. K. Kanaujia, and A. Kumar, "A compact modified Sierpinski carpet fractal UWB MIMO antenna with square-shaped funnel-like ground stub," *AEU — International Journal of Electronics and Communications*, 153126, 2020.
31. Banerjee, J., A. Karmakar, R. Ghatak, and D. R. Poddar, "Compact CPW-fed UWB MIMO antenna with a novel modified Minkowski fractal Defected Ground Structure (DGS) for high isolation and triple band-notch characteristic," *Journal of Electromagnetic Waves and Applications*, Vol. 31, No. 15, 1550–1565, 2017.
32. Althuwayb, A. A., "Low-interacted multiple antenna systems based on metasurface-inspired isolation approach for MIMO applications," *Arab. J. Sci. Eng.*, Vol. 47, 2629–2638, 2022.
33. Alibakhshikenari, M., E. M. Ali, M. Soruri, et al., "A comprehensive survey on antennas on-chip based on metamaterial, metasurface, and substrate integrated waveguide principles for millimeter-waves and terahertz integrated circuits and systems," *IEEE Access*, Vol. 10, 3668–3692, 2022.
34. Shrivishal, T., M. Akhilesh, and Y. Sandeep, "A compact octagonal fractal UWB MIMO antenna with WLAN band-rejection," *Microwave and Optical Technology Letters*, Vol. 57, No. 8, 1919–1925, 2015.
35. Tripathi, S., A. Mohan, and S. Yadav, "A compact Koch fractal UWB MIMO antenna with WLAN band-rejection," *IEEE Antennas and Wireless Propagation Letters*, Vol. 14, 1565–1568, 2015.
36. Rekha, V. S. D., P. Pardhasaradhi, B. T. P. Madhav, and Y. U. Devi, "Dual band notched orthogonal 4-element MIMO antenna with isolation for UWB applications," *IEEE Access*, Vol. 8, 145871–145880, 2020.
37. Sharma, M., V. Dhasarathan, S. K. Patel, and T. Khang Nguyen, "An ultra-compact four-port 4×4 superwideband MIMO antenna including mitigation of dual notched bands characteristics designed for wireless network applications," *International Journal of Electronics and Communications*, Vol. 123, 153332, 2020.
38. Raheja, D. K., B. K. Kanaujia, and S. Kumar, "Compact four-port MIMO antenna on slotted-edge substrate with dual-band rejection characteristics," *Int. J. RF Microw. Comput. Aided Eng.*, e21756, 2019.
39. Verdhan Singh, H. and S. Tripathi, "Compact UWB MIMO antenna with fork-shaped stub with Vias Based Coupling Current Steering (VBCCS) to enhance isolation using CMA," *International Journal of Electronics and Communications*, Vol. 129, 153550, 2021.
40. Gómez-Villanueva, R. and H. Jardón-Aguilar, "Compact UWB uniplanar four-port MIMO antenna array with rejecting band," *IEEE Antennas and Wireless Propagation Letters*, Vol. 18, No. 12, 2543–2547, December 2019.
41. Tripathi, S., A. Mohan, and S. Yadav, "A compact Koch fractal UWB MIMO antenna with WLAN band-rejection," *IEEE Antennas and Wireless Propagation Letters*, Vol. 14, 1565–1568, 2015.
42. Alam, T., S. R. Thummaluru, and R. K. Chaudhary, "Integration of MIMO and cognitive radio for sub-6 GHz 5G applications," *IEEE Antennas and Wireless Propagation Letters*, Vol. 18, No. 10, 2021–2025, October 2019.

43. Saxena, G., Y. K. Awasthi, and P. Jain, "Four-element pentaband MIMO antenna for multiple wireless application including dual-band circular polarization characteristics," *International Journal of Microwave and Wireless Technologies*, 1–12, 2021.
44. Yin, W., S. Chen, J. Chang, C. Li, S. K. Khamas, "CPW fed compact UWB 4-element MIMO antenna with high isolation," *Sensors*, Vol. 21, No. 8, 2688, 2021.
45. Alibakhshikenari, M., B. S. Virdee, I. C. See, R. A. Abd-Alhameed, F. Falcone, A. Andújar, J. Anguera, and E. Limiti, "Study on antenna mutual coupling suppression using integrated metasurface isolator for SAR and MIMO applications," *2018 48th European Microwave Conference (EuMC)*, 1425–1428, Madrid, Spain, September 25–27, 2018.
46. Mark, R., N. Mishra, K. Mandal, P. Pratim Sarkar, and S. Das, "Hexagonal ring fractal antenna with dumb bell shaped defected ground structure for multiband wireless applications," *International Journal of Electronics and Communications*, Vol. 94, 42–50, 2018.
47. Thummaluru, S. R., M. Ameen, and R. K. Chaudhary, "Four-port MIMO cognitive radio system for midband 5G applications," *IEEE Transactions on Antennas and Propagation*, Vol. 67, No. 8, 5634–5645, August 2019.
48. Sharawi, M. S., "Printed multi-band MIMO antenna systems and their performance metrics," *IEEE Antennas Propag. Mag.*, Vol. 55, No. 5, 219–232, 2013.
49. Naik, M. N. and H. G. Virani, "A compact four port MIMO antenna for millimeterwave applications," *Bulletin of Electrical Engineering and Informatics*, Vol. 11, No. 2, 2022.
50. Karaboikis, M. P., V. C. Papamichael, G. F. Tsachtsiris, C. F. Soras, and V. T. Makios, "Integrating compact printed antennas onto small diversity/MIMO terminals," *IEEE Trans. Antennas Propag.*, Vol. 56, No. 7, 2067–2078, 2008.